Multidrug Resistance Protein (MRP) 1 and MRP3 Attenuate Cytotoxic and Transactivating Effects of the Cyclopentenone Prostaglandin, 15-Deoxy-$\Delta^{12,14}$Prostaglandin J_2 in MCF7 Breast Cancer Cells†

Christian M. Paumi,‡ Marcus Wright,§ Alan J. Townsend,‡ and Charles S. Morrow*,‡

Department of Biochemistry, Wake Forest University School of Medicine, Medical Center Boulevard, and Department of Chemistry, Wake Forest University, Winston-Salem, North Carolina 27157

Received December 12, 2002

ABSTRACT: One of the most potent cyclopentenone prostaglandins, 15-deoxy-$\Delta^{12,14}$prostaglandin J_2 (15-d-PGJ_2), has been shown to be cytotoxic in some tumor cells and, as a ligand of peroxisome proliferator activated receptor γ (PPARγ), to influence the transcriptional regulation of several genes. We examined whether a glutathione conjugate of 15-d-PGJ_2, 15-d-PGJ_2−SG, is formed and if the glutathione conjugate efflux pumps, MRP1 and MRP3, could transport this conjugate, thereby attenuating the cytotoxicity and transactivating activity of 15-d-PGJ_2 in MCF7 breast cancer cells. Formation of 15-d-PGJ_2−SG was demonstrated both in vitro and in cells, and its structure was determined by ESI/MS and NMR. Expression of MRP1 and MRP3 was achieved by stable transduction of parental MCF7 cells. Membrane vesicles derived from these cells supported efficient, ATP-dependent transport of 15-d-PGJ_2−SG (K_M 1.4 and 2.9 μM for MRP1 and MRP3, respectively). When compared with parental, MRP-minus MCF7 cells, expression of MRP1 and MRP3 conferred ∼2-fold protection from 15-d-PGJ_2 cytotoxicity. 15-d-PGJ_2-mediated transcriptional activation was evaluated in cells transiently transfected with a reporter gene under the transcriptional control of a PPAR responsive element. Treatment of parental MCF7 cells with 15-d-PGJ_2 resulted in a time-dependent induction of reporter gene activity—induction that was measurable with concentrations of added 15-d-PGJ_2 as low as 100 nM. In contrast, expression of MRP1 or MRP3 abolished 15-d-PGJ_2-dependent reporter gene induction. Depletion of intracellular glutathione reversed MRP1- and MRP3-mediated attenuation of 15-d-PGJ_2 cytotoxicity and transactivation. These data indicate that MRP1 and MRP3 can modulate the biological effects of 15-d-PGJ_2, and likely other cyclopentenone prostaglandins, in a glutathione-dependent manner. The results are consistent with a mechanism for the attenuation of the biological activities of 15-d-PGJ_2 that involves the formation and active efflux of its glutathione conjugate, 15-d-PGJ_2−SG.

The cyclopentenone prostaglandins (CP-PG)[1] affect a variety of cellular processes including growth and differentiation, gene expression, and apoptosis (*1*−*6*). 15-d-PGJ_2, the most potent of the J-series CP-PG, is derived from PGD_2 by dehydration and isomerization reactions (*5*, *7*−*11*). 15-d-PGJ_2 has attracted considerable attention because of its antitumor activities including the ability to inhibit growth and induce apoptosis in several cancer cell lines (*3*, *12*−*16*). Additionally, 15-d-PGJ_2 influences the expression of several genes and has antiinflammatory effects (*5*, *8*, *17*−*21*).

15-d-PGJ_2 is a key end-product of PGD_2 metabolism. In addition to its potential pharmacological utility, the physiological relevance of 15-d-PGJ_2 is supported by recent findings showing that it is produced in cells and tissues including activated macrophages, where 15-d-PGJ_2 is made and secreted (*22*), and human breast tissue (*23*).

The potent biological effects of 15-d-PGJ_2 are mediated by both PPARγ-dependent and -independent mechanisms. PPARγ is a nuclear receptor that, as a heterodimer with the retinoid X receptor (RXR), regulates gene expression via interaction with the DNA responsive element, PPRE (*24*−*26*). As a ligand of PPARγ, 15-d-PGJ_2 activates PPARγ facilitating its dimerization with RXR and the recruitment of co-activators of transcription (*5*, *7*, *8*, *27*, *28*). Additionally, some 15-d-PGJ_2 activities are believed to operate independently of PPARγ via mechanisms that depend on the

† This work was supported by NIH Grant CA70338 (CSM) and a NIEHS predoctoral award TS ES07331 (CMP).

* To whom all correspondence should be sent to Department of Biochemistry, Wake Forest University School of Medicine Medical Center Boulevard, Winston-Salem, NC 27157. Telephone: 336−713−7218. Fax: 336−716−7671, E-mail: cmorrow@wfubmc.edu.

‡ Department of Biochemistry, Wake Forest University School of Medicine.

§ Department of Chemistry, Wake Forest University.

[1] Abbreviations: BSO, L-buthionine-(*S*,*R*)-sulfoximine; CID, collision induced dissociation; CP-PG, cyclopentenone prostaglandins; DMEM, Delbecco's modified Eagle medium; ESI, electrospray ionization; 15-d-PGJ_2, 15-deoxy-$\Delta^{12,14}$prostaglandin J_2; 15-d-PGJ_2−SG, glutathione conjugate of 15-d-PGJ_2; HPLC, high performance liquid chromatography; IC_{50}, drug concentration at which cell proliferation is inhibited 50% of control; MRP, multidrug resistance protein; MS, mass spectroscopy; 9,10-dihydro-15-d-PGJ_2, 9,10-dihydro-15-deoxy-$\Delta^{12,14}$prostaglandin J_2; PCA, perchloric acid; PPARγ, peroxisome proliferator activated receptor γ; PPRE, peroxisome proliferator activated receptor responsive element; PGA_2−SG, glutathione conjugate of prostaglandin A_2; PGJ_2−SG, glutathione conjugate of prostaglandin J_2.

10.1021/bi027347u CCC: $25.00
Published on Web 04/18/2003

reactivity of its electrophilic α,β-unsaturated ketone (*18*, *19*, *29*, *30*). Indeed, the inhibition of cell proliferation by CP-PG has been attributed to the presence of this α,β-unsaturated carbonyl in a variety of tumor models (*1*, *2*). Moreover, previous studies have indicated that this electrophilic center of 15-d-PGJ_2 and other CP-PG is a target for the Michael addition of glutathione (*1*, *31*−*34*). Accordingly, we determined whether a glutathione conjugate of 15-d-PGJ_2 was formed under physiological conditions and whether glutathione-conjugate efflux transporters (*35*, *36*), MRP1 (ABCC1) and MRP3 (ABCC3), could transport the conjugate thereby attenuating biological effects of 15-d-PGJ_2 treatment in MCF7 breast cancer cells.

MCF7 cells lack MRP but express PPARγ and are sensitive to the cytotoxicity of 15-d-PGJ_2 (*12*, *37*). To examine the influence of glutathione conjugate transporters on the cellular effects of 15-d-PGJ_2, MCF7 cells were stably transduced with expression vectors encoding MRP1 and MRP3. The results indicate that MRP1 and MRP3 can attenuate both the transactivating and cytotoxic activites of 15-d-PGJ_2. This attenuation was glutathione-dependent and was associated with the ability of MRP1 and MRP3 to transport the glutathione conjugate, 15-d-PGJ_2−SG, efficiently.

EXPERIMENTAL PROCEDURES

In Vitro Preparation and Analysis of the Glutathione Conjugate of 15-d-PGJ_2 (15-PGJ_2−SG). 15-d-PGJ_2−SG or PGA_2−SG were prepared in 1−5 mL solutions containing 1 mM 15-d-PGJ_2 or PGA_2 (Cayman Chemical, Ann Arbor, MI), 10 mM glutathione (GSH) (Sigma, St. Louis, MO), 140 mM KCl, and 0.1 M sodium phosphate (pH 7.5) at 37 °C for 30 min. The reaction was stopped by the addition of 70% perchloric acid (PCA) to a final concentration of 5% PCA. For analytical HPLC, samples from these conjugation reactions with PGA_2 or 15-d-PGJ_2 were injected onto a Rainin Rabbit-HPX HPLC system (solvent A: 35% acetonitrile, 0.05%TFA, solvent B: 100% acetonitrile) and eluted isocratically for 30 min in solvent A followed by a 20 min gradient (0−60% solvent B). For electrospray mass spectrometry and NMR, 15-d-PGJ_2−SG was purified from reaction mixtures as follows: samples were loaded onto Waters (Milford, MA) Oasis HLB 3-cc extraction cartridges prewashed with 10 mL of methanol followed by 10 mL of 50 mM ammonium acetate (pH 3.0). The loaded cartridge was then washed sequentially with 10 mL of 50 mM ammonium acetate (pH 3.0) and 10 mL of heptane. 15-d-PGJ_2−SG was eluted from the column by 10 mL of 35% acetonitrile containing 0.05% trifluoracetic acid (TFA). The eluate was evaporated to a volume of ∼200 μL under N_2 and further purified by HPLC using the same system described above. The peak fraction containing 15-d-PGJ_2−SG (elution time 34.5 min) was collected and snap frozen in a dry ice/acetone bath. The sample was then lyophilized overnight. The lyophilized powder was resuspended in 700 μL of D_2O and 2 μL of 12 N DCl for NMR analysis (500 MHz Bruker NMR). Alternatively, eluate from the Oasis HLB cartridge was directly analyzed by HPLC or electrospray mass spectroscopy.

All NMR spectra were collected on a Bruker 500 DRX equipped with a 5-mm triple resonance broadband inverse probe. Data collection was at 298 K in 99.9% D_2O in a 2-mm NMR tube. The 1-D ^1H spectrum was collected with 128 scans using double-pulsed field gradient water suppression (DPFGSE-WATERGATE) (*38*). The 2-D DQF-COSY spectrum was collected with 2048 points in the F2 dimension and 512 points in the F1 dimension with 64 scans per time increment. The ^1H 2-D spectral width was 10 ppm centered on the water resonance. Processing ^1H 2-D spectrum consisted of making both F2 and F1 dimensions 2048 points. The H8−H9 coupling constant was extracted from the active coupling associated with the H8−H9 cross-peak. Modeling of both diastereomers was carried out in 02 SPATAN ES (Wave function Inc., Irvine, CA). A semiempirical AM1 geometry optimization was carried out on both diastereomers from several different starting structures (*39*). The H8−H9 dihedral angles for both diastereomers were measured and the coupling constants were calculated with electronegativity parameters (*40*−*42*). The measured and calculated H8−H9 coupling constants were then compared.

Radiolabeled 15-d-PGJ_2−SG was prepared in a total reaction volume of 200 μL containing 6 mM 15-d-PGJ_2, 1.01 mM GSH (specific activity of 0.51 Ci/mmol) [*glycine-2*-^3H] glutathione (PerkinElmer Life Sciences), 0.1 M sodium phosphate (pH 7.8), and 0.2 M NaCl. The reaction mixture was incubated at 37 °C for 30 min and then terminated by the addition of PCA to a final concentration of 5%. The radiolabeled conjugate ([^3H]-15-d-PGJ_2−SG) was purified by HPLC and lyophilized. The lyophilized powder was redissolved in 10 mM Tris (pH 7.5) for use in inside−out vesicle transport studies.

Cell Lines and Culture. All cell lines were derived from parental MCF7 cells (MCF7/WT) and were grown in Dulbecco's modified Eagle medium (DMEM) supplemented with 10% fetal bovine serum (FBS) at 37 °C, 5% CO_2. For some experiments, a drug-selected multidrug resistant derivative cell line expressing MRP1, MCF7/VP, was used (*43*). Transgenic MCF7 cells expressing MRP1 (MCF7/MRP1−10) and MRP3 (MCF7/MRP3−9) were obtained as follows. The cDNAs encoding human MRP1 and MRP3 (see below) were inserted into the multiple cloning site of pLNCX (*44*). These vectors were stably expressed in MCF7 cells by retroviral transduction as described (*44*). Briefly, expression vectors were transiently transfected into PA317 amphotropic packaging cells and the resulting viral supernatants were used to transduce MCF7 cells. MRP expressing clones were selected in 1 mg/mL G418. Cells were maintained in 0.5 mg/mL G418 until 3 days prior to experiments when drug was removed. MRP expression was verified by Northern (*45*, *46*) and Western blot (*45*, *47*) as described previously using the QCRL1 (MRP1) and MRP3 II-9 (MRP3) antibodies from Alexis Biochemicals (Carlsbad, CA).

The cDNA for MRP1 was derived from pJ3Ω-MRP, a plasmid kindly supplied by Guido Zaman (*48*). Using restriction endonuclease cleavage and PCR, the cDNA was truncated to exclude all but the coding and Kozak consensus sequences prior to insertion into pLNCX. The MRP3 cDNA was obtained by PCR amplification of a first strand cDNA synthesized from human liver mRNA (Clontech, Palo Alto, CA) using AMV reverse transcriptase (*49*). A 4628-bp fragment containing the entire coding region of MRP3 was amplified using the Expand High Fidelity DNA polymerase mixture (Roche, Indianapolis, IN) according to the manu-

facturer's recommendations. The 5′-oligonucleotide used, 5′-AAGCCACCATGGACGCCCTGTGCGGTTCC-3′, was modified from the published sequence (modified bases underlined) to create a perfect Kozak consensus (*50*). The 3′-oligonucleotide was 5′-CCAGGAAAGGCCAGGAG-GAAATCTCAGGAA-3′. The veracity of the amplified DNA was ascertained by sequence analysis (DNA Synthesis Core Laboratory, Comprehensive Cancer Center of Wake Forest University) and comparison with the published database sequences (Genbank accession numbers AB10887 and Y17151).

Cytoxicity experiments were performed using the sulforhodamine B microtiter plate assay as previously described with the following modifications (*51, 52*). Cytotoxicity experiments were performed ± BSO (Sigma, St. Louis, MO) to evaluate the effects of glutathione depletion on MRP-mediated resistance to 15-d-PGJ_2 cytoxicity. Total GSH was measured as described (*53*). Cells were plated at either 100 cells/well (+BSO) or 300 cells/well (−BSO) in DMEM containing 10% FBS. Cells were exposed to varying amounts of methotrexate (Sigma, St. Louis, MO), 15-d-PGJ_2, or 9,-10-dihydro-15-deoxy-$\Delta^{12,14}$-prostaglandin J_2 (9,10-dihydro-15-d-PGJ_2) (Cayman, Ann Arbor, MI) for 1 (15-d-PGJ_2 or 9,10-dihydro-15-d-PGJ_2) or 4 h (methotrexate) in serum-free DMEM medium. Following drug exposure, cells were briefly washed with 80 μL of serum-free DMEM and medium containing 10% FBS was replaced.

Analysis of 15-d-PGJ_2−SG Formation in MCF7 Cells. Parental MCF7 cells (4×10^6 cells in 2 100-mm tissue culture dishes) were treated in serum-free DMEM containing 20 μM 15-d-PGJ_2 or equivalent ethanol vehicle control. Following 1 h (37 °C, 5% CO_2) incubation, cells were washed with PBS to remove extracellular 15-d-PGJ_2, scraped in PBS, and pelleted at 500*g* for 5 min. Cell pellets were suspended in serum-free DMEM and 0.38 mL of 70% perchloric acid was added. The suspension was extracted as described (*54*). Briefly, the suspension was extracted twice with 5 mL of ethyl acetate. The aqueous phase was applied to an Oasis HLB 3 cm^3 extraction cartridge and washed with ammonium acetate solution and heptane as described above. Material eluting in 10 mL of 95% ethanol was dried under N_2 to 100 μL and used for HPLC tandem mass spectrometry analysis.

HPLC/ESI/MS/MS. HPLC was with a Hewlett-Packard 1100 equipped with a Hypersil ODS−BD 3 μM, 2.0 × 150 mm column (Phenomenex, Torrence, CA). The mobile phase consisted of 33% acetonitrile, 0.05% trifluoroacetic acid (solvent A), and 100% acetonitrile (solvent B). Samples (50 μL) derived from cell extracts (above) were chromatographed at 200 μL/min before entering the electrospray source. HPLC separation began at 100% solvent A (5 min) followed by a linear gradient to 70% solvent B (15 min) which was then held at 70% B for 5 min. Approximately 12% of the HPLC eluate was diverted to the electrospray source. MS/MS analysis was accomplished using a Micromass Quattro II mass spectrometer equipped with a z spray source and triple quadrupole analyzer. The instrument was operated in positive ion mode with the capillary voltage set to 3.5 kV and the sampling cone to 35 V. The argon gas pressure was set to 1 microbar and the collision energy was 20 eV.

Preparation of Inside−Out Plasma Membrane Vesicles and Determination of MRP1- and MRP3-Dependent Conjugate Uptake. Membrane vesicles were prepared from parental (MCF7/WT) and transduced (MCF7/MRP1−10 and MCF7/MRP3−9) cells as described previously (*55*). The kinetics of ATP-dependent [^{3}H]-methotrexate (Moravek, Brea, CA) or [^{3}H]-15-d-PGJ_2−SG uptake was determined as described except that 10 mM creatine phosphate and 100 μg/mL creatine kinase (Roche, Indianapolis, IN) were included in the reaction mixtures (*55*). Kinetic constants were calculated from the initial velocities of ATP-dependent uptake that were fitted to the Michaelis−Menten equation using Synergy KaleidaGraph 3.5 software for the Macintosh.

PPARγ-Dependent Transactivation Assays. Cells were plated at a density of 0.75×10^5 cells per well in six-well dishes and grown for 24 h at 37 °C, 5% CO_2. Cells were then transfected with 1 μg of PPREx3-TK-LUC plasmid (*8*) (kindly supplied by Dr. Ronald Evans, Salk Institute). The PPREx3-TK-LUC plasmid contains three PPARγ response elements (PPRE) inserted upstream of a thymidine kinase promoter driving transcription of a firefly luciferase gene. Cells were transfected using Superfect transfection reagent (Qiagen, Valencia, CA). Twenty-four hours after transfection with PPREx3-TK-LUC, the cells were treated with 0.1−20 μM 15-d-PGJ_2, 30 μM 9,10-dihydro-15-d-PGJ_2, or vehicle in 3 mL of serum-free DMEM for 1 h. Medium containing vehicle or compound was removed, cells were washed once with PBS, and 3 mL of fresh DMEM containing 10% FBS was replaced. Transfected cells were harvested at timed intervals 0, 3, 6, 9, 12, 15, 24, and 29 h following the completion of treatment with vehicle or compound. Luciferase activity was determined using the Promega Luciferase Assay kit (Promega, Madison, WI) and a Turner TD-20e luminometer.

RESULTS

Formation and Structure of 15-d-PGJ_2−SG. Incubation of 15-d-PGJ_2 with glutathione under physiological conditions resulted in the formation of a single derivative resolved by HPLC (Figures 1 and 2). This derivative, eluting at 34.5 min (Figure 2A), was identified as a monoglutathionyl conjugate of 15-d-PGJ_2 (15-d-PGJ_2−SG) by electrospray mass spectroscopy (*m*/*z* 624, $M+H^+$). Moreover, under chromatographic conditions that resolve the two diastereomers reported for PGA_2−SG (insert, Figure 2B) (*32*), only one peak is observed for 15-d-PGJ_2−SG. While these data indicate that glutathione conjugation probably occurs stereoselectively at a single carbon—most likely at the ketone conjugated, unsaturated C9 position (Figure 1)—definitive assignment of the site and stereochemistry of glutathione conjugation was accomplished by NMR.

NMR analysis, ^{1}H NMR, and DQF−COSY (Table 1, Figure 3), allowed complete assignment of the 15d-PGJ_2−SG conjugate. The site of conjugation was identified by mapping three distinctly separate spin systems: (i) glutathione, (ii) C1 to C10, and (iii) C12 to C20. Analysis of COSY spectra confirmed that the coupling pattern between H13, 14, and 15 was conserved indicating that Michael addition of glutathione must have occurred elsewhere in the molecule. Loss of the characteristic α,β-unsaturated H9−H10 spins in 15d-PGJ_2−SG offered further support for the conclusion that conjugation occurred at C9. Alkene proton H6 clearly showed coupling to two diastereotopic protons

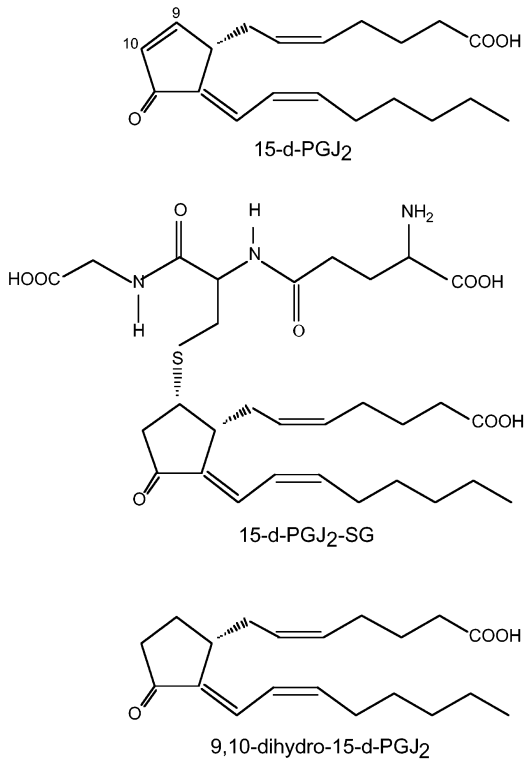

FIGURE 1: Structures of 15-d-PGJ_2, 15-d-PGJ_2−SG, and 9,10-dihydro-15-d-PGJ_2. The structure of 15-d-PGJ_2−SG was determined by HPLC/electrospray mass spectrometry and by ^{1}H, P-COSY, and DQF-COSY NMR spectroscopy as described in Experimental Procedures and Results. The structures of 15-d-PGJ_2 and its 9,10-dihyro analogue are shown for reference.

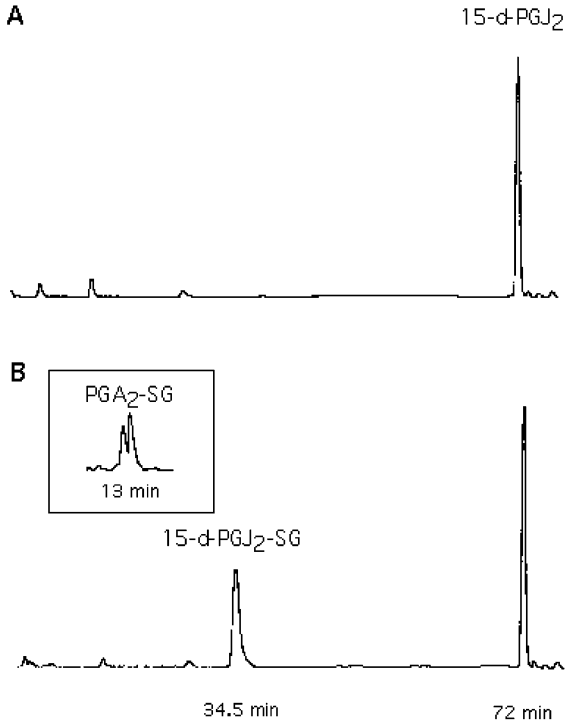

FIGURE 2: Analytical HPLC of 15-d-PGJ_2 and its glutathione conjugate, 15-d-PGJ_2−SG. Reactions containing 15-d-PGJ_2 (A, −glutathione; B, +glutathione) were examined by HPLC as described in Experimental Procedures. The parent compound elutes at 72 min (A and B) and the monoglutathionyl conjugate at 34.5 min (B). The structure of this conjugate, 15-d-PGJ_2−SG, was determined by mass spectrometry and NMR. Additionally, a reaction containing PGA_2 and glutathione was analyzed by HPLC. Resolution of the two reported diastereomers of PGA_2−SG (*32*) formed is shown in the inset (B).

H7a and H7b. These protons were then seen to couple to a single proton, H8, which in turn was coupled to a proton at 4.63 ppm, H9. The proton assigned to H9 was coupled to two diasterotopic protons, H10a and H10b. The coupling and chemical shifts were consistent with conjugation at C9. Once the assignments were made, the H8 to H9 coupling constant was measured from the DQF-COSY active coupling (Figure 3) and compared to calculated coupling constants for the syn and anti addition products of 15d-PGJ_2−SG. The *J* values were calculated by energy minimizing the syn and anti structures in 02 SPATAN ES (Wave function Inc., Irvine, CA) then measuring the resulting H8−H9 dihedral angles (47 and 170 degrees for the syn and anti structures, respectively). Using the dihedral angles in an electronegativity adapted Karpulus equation, a value of 4.3 Hz for the syn product and 11 Hz for the anti product was calculated (*40*−*42*). The measured *J* value of 5 Hz agreed with the calculated *J* value of 4.3 Hz for the syn addition product. By inspection of the NMR data, we did not detect any appreciable amount of the anti addition product.

Formation of 15-d-PGJ_2−SG from Exogenous and Endogenous 15-d-PGJ_2 in MCF7 Cells. Having established that 15-d-PGJ_2−SG forms in vitro, it was necessary to determine whether the conjugate was formed in intact cells. MCF7/WT cells were treated for 1 h with 20 μM 15-d-PGJ_2 or vehicle control. Cellular extracts were prepared and analyzed by HPLC/ESI/MS/MS as described in Experimental Procedures. These results are displayed in the multiple reaction-monitoring chromatograms shown in Figure 4. The precursor ion *m*/*z* 624, corresponding to 15-d-PGJ_2−SG, was selected for all analyses. Product ions corresponding to the glutathione and prostaglandin CID fragments of 15-d-PGJ_2−SG were scanned at *m*/*z* 308 (panels A and B) and 317 (panels C and D), respectively. Using these parameters, the chromatograms in Figure 4 show a single major peak (HPLC retention ∼ 15 min) and demonstrate that 15-d-PGJ_2−SG is formed in intact cells. Moreover, the data show that 15-d-PGJ_2−SG is made from both exogenously added (Figure 4, panels B and D) and endogenous (Figure 4, panels A and C) sources

Table 1: Proton Chemical Shift Data for 15-d-PGJ_2[a]

^{1}H resonance	chemical shift (ppm)
2	2.39
3	1.69
4	2.11
5	5.55
6	5.48
7a,b	2.24, 2.38
8	3.00
9	4.63
10a,b	2.89, 3.10
13	6.99
14	6.34
15	6.29
16	2.22
17	1.47
18	1.34
19	1.34
20	0.92

[a] 15-d-PGJ_2 was analyzed by ^{1}H NMR and DQF-COSY NMR spectroscopy as described in Experimental Procedures. Chemical shifts determined for individual protons are listed.

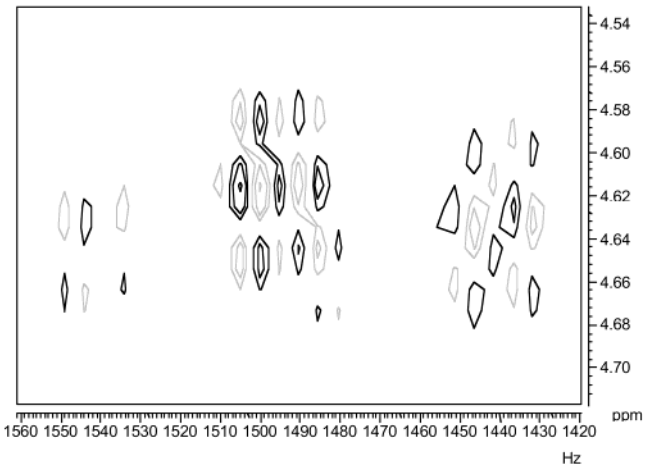

FIGURE 3: DQF-COSY showing coupling between H9 and H8 on 15d-PGJ$_2$−SG. DQF-COSY NMR spectroscopy was carried out as described in Experimental Procedures. Displayed is a 500 MHz DQF-COSY showing the H8 (1495 Hz) to H9 (4.64 ppm) cross-peak. Positive contours are indicated by black, and negative contours are indicated by gray. The active coupling constant was measured from the H8−H9 cross-peak. The measured coupling constant of 5 Hz was consistent with the calculated coupling constant of 4.3 Hz for the energy minimized syn addition structure (anti-addition structure gave a H8−H9 $J = 11$ Hz).

of 15-d-PGJ$_2$. However, comparison of the relative ion current intensities indicates that at least 100-fold more conjugate is present in MCF7/WT cells treated with 20 μM 15-d-PGJ$_2$ (B and D) than in untreated control cells (A and C).

Characterization of MRP-Transduced Cell Lines. While parental MCF7/WT cells do not express MRP1 or MRP3 (*45*, *46*, *56*), stable transduction of MRP expression vectors resulted in high levels of MRP1 and MRP3 in MCF7/MRP1−10 and MCF7/MRP3−9 cells, respectively. Functional characterization of MCF7/MRP1−10 will be reported elsewhere. Briefly, MRP1 is highly expressed on the plasma membrane of MCF7/MRP1−10 cells. Vesicles derived from these cells support ATP-dependent transport of several glutathione conjugates and of methotrexate (Table 2). Last, MRP1 expression in MCF7/MRP1−10 cells confers resistance to the cytotoxicities of several drugs associated with the MRP1 resistance phenotype including doxorubicin (10-fold resistance) and etoposide (8-fold resistance).

Cells transduced with MRP3, MCF7/MRP3−9, express both MRP3 RNA and plasma membrane-associated protein (Figure 5). Vesicles derived from these cells demonstrate ATP-dependent methotrexate transport (Table 2). Moreover, expression of MRP3 confers 3-fold resistance to the cytotoxicity of methotrexate (1 h drug exposure, data not shown).

MRP1 and MRP3 Transport 15-d-PGJ$_2$−SG. Inside−out membrane vesicles derived from MRP1 (MCF7/MRP1−10) and MRP3 (MCF7/MRP3−9) expressing cells support efficient ATP-dependent transport of 15-d-PGJ$_2$−SG, whereas membranes from parental (MCF7/WT) cells do not (Figure 6). Similar K_m values of 1.4 and 2.9 μM were observed, respectively, for MRP1 and MRP3 (Table 2).

The efficiency and capacity for substrate transport depend on the cellular levels as well as the inherent properties of the MRP expressed. The transport kinetics of a known common substrate of the two transporters, methotrexate (*57*−*59*), were compared with those of 15-d-PGJ$_2$−SG. This approach allowed some adjustment for potentially different levels of protein expression. From these data (Table 2), the relative efficiency and capacity of 15-d-PGJ$_2$−SG transport by MRP1 and MRP3 was ascertained. As shown, both MRP1 and MRP3 supported methotrexate transport with similar K_m values of 0.93 and 0.91 mM, respectively. The V_{max} was higher in MRP1-expressing cells resulting in a 2-fold higher efficiency of transport (V_{max}/K_m). Similar calculations for 15-d-PGJ$_2$−SG transport were made and normalized for differences in the efficiency of methotrexate transport observed

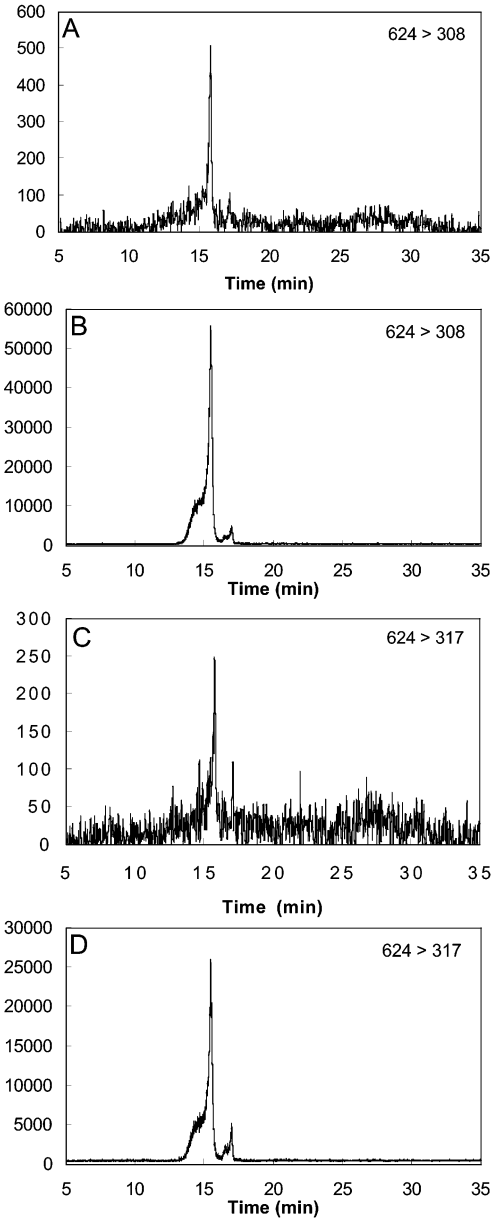

FIGURE 4: 15-d-PGJ$_2$−SG formation in MCF7 cells. 15-d-PGJ$_2$−SG formation was analyzed in extracts of MCF7 cells treated with 20 μM 15-d-PGJ$_2$ (panels B and D) or vehicle control (panels A and C). Multiple reaction-monitoring HPLC/ESI/MS/MS chromatograms are shown with ion current intensities expressed as equivalent arbitrary units (ordinate). The precursor ion corresponding to 15-d-PGJ$_2$−SG at *m*/*z* 624 was selected in all chromatograms. Product ions were scanned at *m*/*z* 308 (glutathione fragment, panels A and B) and at *m*/*z* 317 (prostaglandin fragment, panels C and D). Panels A and C represent analyses from a single multiple reaction-monitoring run of extracts from control cells. Panels B and D represent chromatograms from a single run of extracts from 15-d-PGJ$_2$-treated cells

Table 2: Kinetics of 15-d-PGJ$_2$−SG and Methotrexate Transport by MRP1 versus MRP3[a]

substrate	K_m (μM)	V_{max} (pmol min^{-1} mg^{-1})	V_{max}/K_m (μL min^{-1} mg^{-1})	relative efficiency[b]
MRP1				
methotrexate	930	380	0.41	1.0
15-d-PGJ$_2$−SG	1.4	67	48	120
MRP3				
methotrexate	910	190	0.21	1.0
15-d-PGJ$_2$−SG	2.9	9.1	3.1	15

[a] Kinetic parameters of methotrexate and 15-d-PGJ$_2$ uptake into inside−out vesicles derived from MRP1 and MRP3 transduced cell lines were determined as described in Experimental Procedures. [b] Relative efficiency of transport is defined for each MRP as V_{max}/K_m divided by V_{max}/K_m of methotrexate.

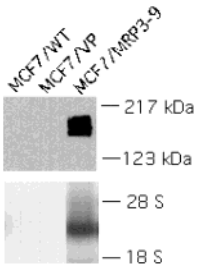

FIGURE 5: MRP3 expression in transduced MCF7 cells. MRP3 expression was analyzed by Western (upper panel) and Northern (lower panel) blots using membrane protein and total RNA preparations, respectively, as described in Experimental Procedures. Material was derived from parental (MCF7/WT); drug selected, MRP1 expressing (MCF7/VP); and transduced, MRP3 expressing (MCF7/MRP3−9) cells.

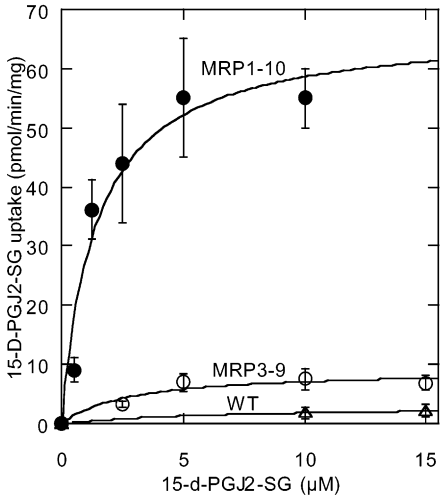

FIGURE 6: ATP-dependent uptake of 15-d-PGJ$_2$−SG by inside−out membrane vesicles derived from MRP1 and MRP3 expressing cells. Shown are the initial velocities of ATP-dependent 15-d-PGJ$_2$−SG uptake by inside−out membrane vesicles prepared from parental (MCF7/WT, WT; triangles), MRP1 expressing (MCF7/MRP1−10, MRP1−10; closed circles), and MRP3 expressing (MCF7/MRP3−9, MRP3−9; open circles) cells. Data points represent the mean values of four replicate determinations ± one standard deviation.

between the two cell lines. Relative efficiency so defined indicates that 15-d-PGJ$_2$−SG is transported 8-fold more efficiently by MRP1 (MCF7/MRP1−10 cells) than by MRP3 (MCF7/MRP3−9 cells) (Table 2).

Expression of MRP1 and MRP3 Modify the Cellular Effects of 15-d-PGJ$_2$. Having established that 15-d-PGJ$_2$ is conjugated with glutathione in cells and that the conjugate,

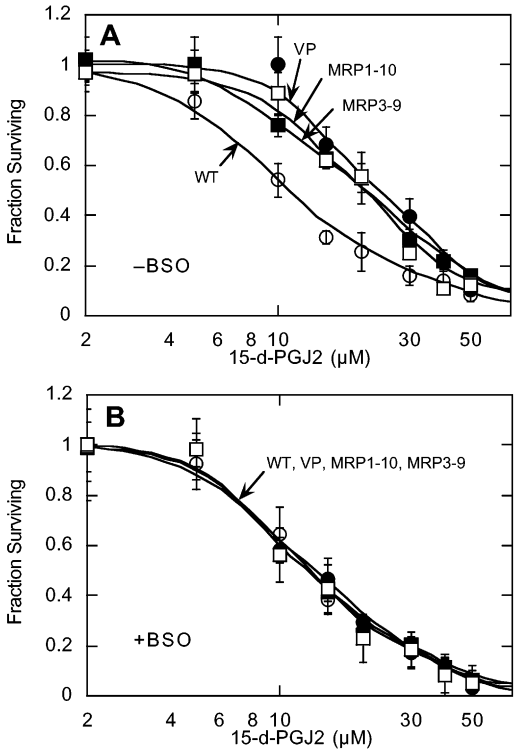

FIGURE 7: MRP1 and MRP3 confer glutathione-dependent resistance to 15-d-PGJ$_2$ cytotoxicity. The cytotoxicity of 15-d-PGJ$_2$ was evaluated in parental (MCF7/WT, WT; open circles), MRP1 expressing (MCF7/MRP1−10, MRP1−10; open squares and MCF7/VP, VP; closed circles), and MRP3 expressing (MCF7/MRP3−9, MRP3−9; closed squares) cell lines as described in Experimental Procedures. Cytotoxicity experiments were done without (A, −BSO) or with (B, +BSO) BSO treatment to deplete intracellular glutathione. BSO treatment resulted in >95% reduction of intracellular glutathione. Data points represent the means of eight replicate determinations ± one standard deviation.

15-d-PGJ$_2$−SG, is efficiently transported by MRP1 and MRP3, we examined whether expression of the MRPs would alter the biological activities of exogenously added 15-d-PGJ$_2$. Cytotoxicity of 15-d-PGJ$_2$ was assessed in cells treated for 1 h with varying concentrations of the compound. As shown in Figure 7A, cytotoxicity of 15-d-PGJ$_2$ is observed in the micromolar range in MCF7 cells. When compared with parental cells (MCF7/WT), expression of MRP1 conferred 2.0−2.1-fold resistance to 15-d-PGJ$_2$ toxicity in both drug-selected (MCF7/VP) and transduced (MCF7/MRP1−10) cells. Similarly, expression of MRP3 (MCF7/MRP3−9) at the levels achieved conferred 2-fold resistance. Depletion of >95% of intracellular glutathione with BSO reversed MRP1- and MRP3-mediated resistance while having no effect on MCF7/WT sensitivity to 15-d-PGJ$_2$ (Figure 7B and Table 3).

Activation of the nuclear receptor and transcription factor, PPARγ, by its ligand 15-d-PGJ$_2$ was examined by transient transfection assay. Cells were transfected with a luciferase reporter gene (PPREx3-TK-LUC) under the transcriptional control of the PPARγ responsive element, PPRE. Transfected cells were treated with 15-d-PGJ$_2$, 9,10-dihydro-15-d-PGJ$_2$, or vehicle control for 1 h and luciferase activity measured at timed intervals thereafter. Results (Figure 8) show that in the absence of MRP expression, treatment of MCF7/WT cells with 20 μM 15-d-PGJ$_2$ resulted in a time-dependent induction

Table 3: Glutathione-Dependent Resistance to 15-d-PGJ_2 Cytotoxicity in MRP1 and MRP3 Expressing Cell Lines

	relative resistance[a]	
cell line	−BSO	+BSO
MCF7/WT	1.0	1.0
MCF7/VP	2.1	1.1
MCF7/MRP1−10	2.0	1.2
MCF7/MRP3−9	2.0	1.2

[a] Relative resistance is defined as the IC_{50}/IC_{50} MCF7/WT − BSO. Data are derived from experiments shown in Figure 7.

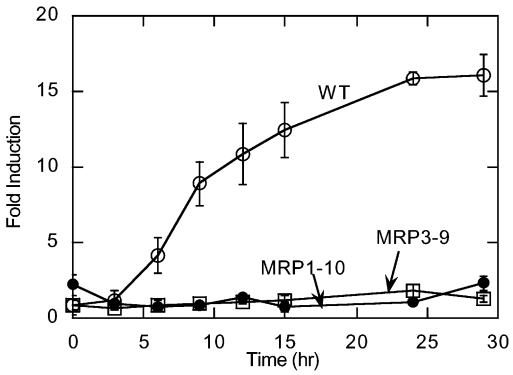

FIGURE 8: MRP1 and MRP3 block 15-d-PGJ_2 induction of PPRE reporter gene expression. The ability of 15-d-PGJ_2 to activate PPARγ and thereby transactivate a PPRE-containing luciferase reporter gene, PPREx3-TK-LUC, was assessed in parental (MCF7/WT, WT; open circles), MRP1 transduced (MCF7/MRP1−10, MRP1−10; closed circles), and MRP3 transduced (MCF7/MRP3−9, MRP3−9; open boxes) cells. As described in Experimental Procedures, cells were transiently transfected with PPREx3-TK-LUC, treated with 20 μM 15-d-PGJ_2 or vehicle for one hr, and were harvested immediately (0 time) or subsequently at indicated timed intervals for reporter gene activity assay. Fold induction is defined as luciferase activity (units/mg of cytosolic protein) in 15-d-PGJ_2-treated cells divided by activity in vehicle-treated control cells. Data points represent the mean values of triplicate determinations ± one standard deviation.

of reporter gene expression that reached 16-fold by 24 h. In contrast, expression of either MRP1 (MCF7/MRP1−10) or MRP3 (MCF7/MRP3−9) virtually abolished induction throughout the time course examined. In MCF7/WT cells, transcriptional activation by 15-d-PGJ_2 was dose-dependent with measurable induction observed with concentrations of exogenously added 15-d-PGJ_2 as low as 100 nM (Figure 9, open bars). Again, expression of MRP1 (MCF7/MRP1−10 cells) abolished 15-d-PGJ_2-mediated induction (Figure 9, shaded bars).

In separate experiments (not shown), the role of glutathione and glutathione conjugate formation in MRP-mediated attenuation of CP−PG-dependent transactivation was investigated. First, depletion of intracellular glutathione by a 48 h preincubation with 50 μM BSO resulted in a 7-fold induction of PPREx3-TK-LUC reporter gene activity in MCF7/MRP1-10 cells upon subsequent treatment with 20 μM 15-d-PGJ_2. This result contrasts with the finding that 15-d-PGJ_2 fails to mediate induction in glutathione replete MCF7/MRP1−10 cells (Figures 8 and 9)—thus indicating that MRP-dependent attenuation of 15-d-PGJ_2-mediated transactivation depends on the presence of physiologic levels of glutathione. Second, treatment of cells with 30 μM of the 15-d-PGJ_2 analogue, 9,10-dihydro-15-d-PGJ_2, which cannot form a glutathione conjugate, stimulated 4-fold induction of

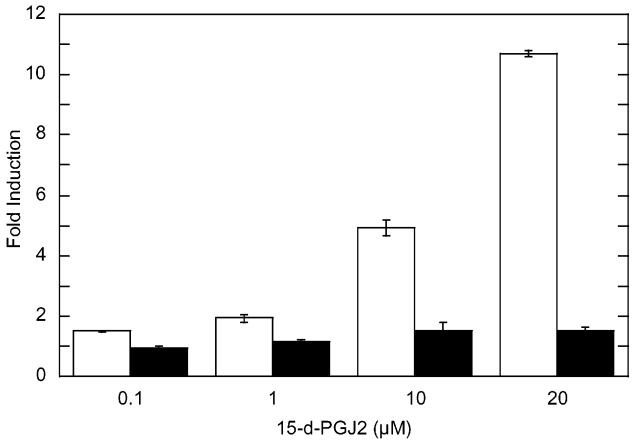

FIGURE 9: MRP1 attenuates 15-d-PGJ_2-mediated induction of PPRE reporter gene expression over a range of 15-d-PGJ_2 concentrations. Parental (MCF7/WT, WT; open bars) and MRP1 transduced (MCF7/MRP1−10. MRP1−10; shaded bars) MCF7 cells were transfected with PPREx3 TK-LUC as described in Figure 8 and Experimental Procedures. Cells were incubated for 1 h with vehicle (control) or the indicated concentrations of 15-d-PGJ_2. 24 h later luciferase activities were measured and fold induction calculated as described in Figure 8. Bars represent mean values of triplicate determinations ± 1 standard deviation.

reporter gene transcription that was unaffected by expression of MRP1 or MRP3.

DISCUSSION

Results presented herein demonstrate that a glutathione conjugate of 15-d-PGJ_2, 15-d-PGJ_2−SG, forms under physiological conditions in vitro (Figures 1−3, Table 1) and in intact cells (Figure 4). Both MRP1 and MRP3 mediate ATP-dependent transport of this conjugate at biologically relevant concentrations (Figure 6, Table 2). Indeed, the K_m of conjugate transport are 1.4 (MRP1) and 2.9 (MRP3) μM and are comparable to the concentrations of parent compound associated with potent biological activities (*3*, *5*, *8*). Expression of either MRP1 or MRP3 attenuated the cellular activities of 15-d-PGJ_2 such that, under the conditions examined, MRP1 and MRP3 conferred ∼2-fold resistance to 15-d-PGJ_2 cytotoxicity (Figure 7, Table 3) and virtually abolished the ability of 15-d-PGJ_2 to transactivate a PPARγ-responsive promoter (Figures 8 and 9).

Structural analysis of 15d-PGJ_2−SG by HPLC, electrospray mass spectrometry, and 1D and 2D NMR confirmed that glutathione is conjugated to 15d-PGJ_2 (Figures 1−3, Table 1). On the basis of the ^{1}H chemical shifts (Table 1), integration, and 2D-DQF-COSY (Figure 3), the site of glutathione thioether attachment was consistent with C9 and not C13 or C15. The relative stereochemistry between glutathione and the C7 tail was consistent with syn addition to C9 when comparing the calculated H8−H9 coupling constants for both the syn (4.3 Hz) and anti (11 Hz) addition products to the DQF−COSY measured coupling constant of 5 Hz. There seem to be fewer van der Waals interactions between the sulfur atom of glutathione and ring protons H8 and H10. This may explain the preferred formation of the syn product. Bogaards et al. have isolated a similar PGJ_2−SG conjugate with the same relative stereochemistry at C9 with similar chemical shifts and coupling constants being observed (*32*).

Using our experimental system, MRP1 (MCF7/MRP1−10 cells) was superior to MRP3 (MCF7/MRP3−9 cells) in supporting 15-d-PGJ_2−SG transport (Figure 6, Table 2). This apparent superiority of MRP1 transport efficiency (V_{max}/K_m) persisted even when data were normalized to the transport efficiency of the common MRP1 and MRP3 substrate, methotrexate (relative efficiency, Table 2). Nevertheless, the levels of MRP1 and MRP3 expressed in these cells resulted in similar levels of cytoprotection (Figure 7) and attenuation of PPRE-containing reporter gene attenuation (Figures 8 and 9). It is possible that under different conditions of 15-d-PGJ_2 exposure or at lower levels of MRP expression, quantitative differences in the affects of MRP1 versus MRP3 expression might have been observed.

The role of glutathione and the importance of glutathione conjugate formation in MRP-mediated modulation of 15-d-PGJ_2 effects were demonstrated. First, depletion of intracellular glutathione by BSO treatment abolished MRP-mediated cytoprotection but had no effect on parental (MRP-minus) MCF7/WT cells (Figure 7). Second, the 15-d-PGJ_2 analogue, 9,10-dihydro-15-d-PGJ_2, does not form a glutathione conjugate, yet it retains some transcriptional transactivating activity. The effect of 9,10-dihydro-15-d-PGJ_2 on PPARγ activation in reporter gene assay was unaffected by MRP1 or MRP3 expression in contrast to the results using 15-d-PGJ_2 as the PPARγ-activating ligand (Figures 8 and 9 and text). Third, depletion of intracellular glutathione with BSO reversed MRP1-dependent attenuation of 15-d-PGJ_2-mediated reporter gene transactivation—a treatment that allowed 7-fold induction of transcription in MCF7/MRP1−10 cells. These results show that MRP1- and MRP3-mediated attenuation of 15-d-PGJ_2 cellular activities is glutathione-dependent. Collectively, they are consistent with attenuation occurring as a consequence of formation of the glutathione conjugate and its subsequent efflux by MRP1 or MRP3. Moreover, the results indicate that glutathione conjugation alone, in the absence of MRP-mediated efflux, is insufficient to completely detoxify 15-d-PGJ_2 (see Figure 7A,B, MCF7/WT ± BSO) or to eliminate 15-d-PGJ_2-stimulated transactivation (Figures 8 and 9, MCF7/WT). The requirement for MRP may be due to the reversibility of the Michael addition of glutathione to 15-d-PGJ_2. Consequently, in the absence of MRP, 15-d-PGJ_2−SG may form and accumulate intracellularly only to be released as the reactive parent compound, 15-d-PGJ_2 by the reverse reaction. In addition, or alternatively, the conjugate may retain some of the PPARγ-binding properties of the parent ligand, 15-d-PGJ_2.

These findings in the MCF7 model cell lines suggest that MRP family proteins may have important biological regulatory effects on 15-d-PGJ_2 action in vivo. Our observations indicate that MRP1 or MRP3 expression may influence activities associated with 15-d-PGJ_2—activities including immunosuppression, local toxicity, differentiation, and gene regulation in normal cells and tissues. Additionally, MRP1 and MRP3 may influence the sensitivities of tumor cells to the cytotoxicity of 15-d-PGJ_2 either secreted as a part of the host response to tumor or administered exogenously as a pharmacological agent. The biological relevance of 15-d-PGJ_2 conjugation and conjugate efflux gains additional support from our findings that 15-d-PGJ_2−SG is indeed formed in intact cells—both from endogenous as well as exogenous sources of 15-d-PGJ_2. It is likely that MRP family members will be generally important in the modulation of biological effects of other eicosanoids that can form glutathione conjugates such as PGA_2, PGJ_2, and Δ^{12}-PGJ_2 (*1*, *31*−*34*).

ACKNOWLEDGMENT

The authors are grateful to Mike Samuel and Dr. Michael Thomas for mass spectroscopy analysis and to Pamela K. Smitherman for expert contributions.

REFERENCES

1. Atsmon, J., Freeman, M., Meredith, M., Sweetman, B., and Roberts, L., 2d. (1990) *Cancer Res. 50*, 1879−1885.
2. Honn, K. V., and Marnett, L. J. (1985) *Biochem. Biophys. Res. Commun. 129*, 34−40.
3. Clay, C. E., Namen, A. M., Fonteh, A. N., Atsumi, G., High, K. P., and Chilton, F. H. (2000) *Prostaglandins & Other Lipid Mediators 62*, 23−32.
4. Clay, C. E., Namen, A. M., Atsumi, G., Trimboli, A. J., Fonteh, A. N., High, K. P., and Chilton, F. H. (2001) *J. Invest. Med. 49*, 413−420.
5. Kliewer, S. A., Lenhard, J. M., Willson, T. M., Patel, I., Morris, D. C., and Lehmann, J. M. (1995) *Cell 83*, 813−9.
6. Rovin, B. H., Wilmer, W. A., Lu, L., Doseff, A. I., Dixon, C., Kotur, M., and Hilbelink, T. (2002) *Kidney Int. 61*, 1293−1302.
7. Dussault, I., and Forman, B. M. (2000) *Prostaglandins & Other Lipid Mediators 62*, 1−13.
8. Forman, B. M., Tontonoz, P., Chen, J., Brun, R. P., Spiegelman, B. M., and Evans, R. M. (1995) *Cell 83*, 803−12.
9. Fitzpatrick, F. A., and Wynalda, M. A. (1983) *J. Biol. Chem. 258*, 11713−8.
10. Kikawa, Y., Narumiya, S., Fukushima, M., Wakatsuka, H., and Hayaishi, O. (1984) *Proc. Natl. Acad. Sci. U.S.A. 81*, 1317−21.
11. Hirata, Y., Hayashi, H., Ito, S., Kikawa, Y., Ishibashi, M., Sudo, M., Miyazaki, H., Fukushima, M., Narumiya, S., and Hayaishi, O. (1988) *J. Biol. Chem. 263*, 16619−25.
12. Clay, C. E., Namen, A. M., Atsumi, G.-i., Willingham, M. C., High, K. P., Kute, T. E., Trimboli, A. J., Fonteh, A. N., Dawson, P. A., and Chilton, F. H. (1999) *Carcinogenesis 20*, 1905−1911.
13. Harris, S. G., and Phipps, R. P. (2002) *Immunology 105*, 23−34.
14. Eibl, G., Wente, M. N., Reber, H. A., and Hines, O. J. (2001) *Biochem. Biophys. Res. Commun. 287*, 522−529.
15. Shimada, T., Kojima, K., Yoshiura, K., Hiraishi, H., and Terano, A. (2002) *Gut 50*, 658−664.
16. Padilla, J., Leung, E., and Phipps, R. P. (2002) *Clin. Immunol. 103*, 22−33.
17. Yamazaki, R., Kusunoki, N., Matsuzaki, T., Hashimoto, S., and Kawai, S. (2002) *J. Pharmacol. Exp. Ther. 302*, 18−25.
18. Rossi, A., Kapahi, P., Natoli, G., Takahashi, T., Chen, Y., Karin, M., and Santoro, M. G. (2000) *Nature 403*, 103−8.
19. Straus, D. S., Pascual, G., Li, M., Welch, J. S., Ricote, M., Hsiang, C.-H., Sengchanthalangsy, L. L., Ghosh, G., and Glass, C. K. (2000) *Proc. Natl. Acad. Sci. U.S.A. 97*, 4844−4849.
20. Ricote, M., Li, A. C., Willson, T. M., Kelly, C. J., and Glass, C. K. (1998) *Nature 391*, 79−82.
21. Jiang, C., Ting, A. T., and Seed, B. (1998) *Nature 391*, 82−6.
22. Shibata, T., Kondo, M., Osawa, T., Shibata, N., Kobayashi, M., and Uchida, K. (2002) *J. Biol. Chem. 277*, 10459−10466.
23. Badawi, A. F., and Badr, M. Z. (2003) *Int. J. Cancer 103*, 84−90.
24. Mangelsdorf, D. J., and Evans, R. M. (1995) *Cell 83*, 841−50.
25. Hihi, A. K., Michalik, L., and Wahli, W. (2002) *Cell. Mol. Life Sci. 59*, 790−798.
26. Kliewer, S. A., Umesono, K., Noonan, D. J., Heyman, R. A., and Evans, R. M. (1992) *Nature 358*, 771−4.
27. Chawla, A., Repa, J. J., Evans, R. M., and Mangelsdorf, D. J. (2001) *Science 294*, 1866−1870.
28. Krey, G., Braissant, O., L'Horset, F., Kalkhoven, E., Perroud, M., Parker, M. G., and Wahli, W. (1997) *Mol. Endocrinol. 11*, 779−791.
29. Cernuda-Morollon, E., Pineda-Molina, E., Canada, F. J., and Perez-Sala, D. (2001) *J. Biol. Chem. 276*, 35530−35536.
30. Castrillo, A., Diaz-Guerra, M. J., Hortelano, S., Martin-Sanz, P., and Bosca, L. (2000) *Mol. Cell Biol. 20*, 1692−8.

31. Atsmon, J., Sweetman, B. J., Baertschi, S. W., Harris, T. M., and Roberts, L. J., 2nd. (1990) *Biochemistry 29*, 3760−5.
32. Bogaards, J. J., Venekamp, J. C., and van Bladeren, P. J. (1997) *Chem. Res. Toxicol. 10*, 310−7.
33. Ohno, K., and Hirata, M. (1993) *Biochem. Pharmacol. 46*, 661−70.
34. Parker, J., and Ankel, H. (1992) *Biochem. Pharmacol. 43*, 1053−60.
35. Borst, P., Evers, R., Kool, M., and Wijnholds, J. (2000) *J. Natl. Cancer Inst. 92*, 1295−302.
36. Keppler, D. (1999) *Free Radical Biol. Med. 27*, 985−991.
37. Elstner, E., Muller, C., Koshizuka, K., Williamson, E. A., Park, D., Asou, H., Shintaku, P., Said, J. W., Heber, D., and Koeffler, H. P. (1998) *Proc. Natl. Acad. Sci. U.S.A. 95*, 8806−11.
38. Hwang, T. L., and Shaka, A. J. (1995) *J. Magn. Res. Ser. A 112*, 275−279.
39. Claridge, T. D. (1999) *High-Resolution NMR Techniques in Organic Chemistry*, Elsevier Science, New York.
40. van Wijk, J., Huckriede, B. D., Ippel, J. H., and Altona, C. (1992) *Methods Enzymol. 211*, 286−306.
41. Haasnoot, C. A. G., DeLeeuw, F. A. A. M., and Altona, C. (1980) *Tetrahedron 36*, 2783−2792.
42. Altona, C., Ippel, J. H., Hoekzem, A. J. A. W., Erkelens, C., Grosbeek, M., and Donders, L. A. (1989) *Magn. Reson. Chem. 27*, 564−576.
43. Schneider, E., Horton, J., Yang, C.-h., Nakagawa, M., and Cowan, K. H. (1994) *Cancer Res. 54*, 152−158.
44. Miller, A. D., Miller, D. G., Garcia, J. V., and Lynch, C. M. (1993) *Methods Enzymol. 217*, 581−599.
45. Morrow, C. S., Diah, S., Smitherman, P. K., Schneider, E., and Townsend, A. J. (1998) *Carcinogenesis 19*, 109−15.
46. Morrow, C. S., Smitherman, P. K., and Townsend, A. J. (2000) *Mol. Carcinog. 29*, 170−178.
47. Hipfner, D. R., Gauldie, S. D., Deeley, R. G., and Cole, S. P. C. (1994) *Cancer Res. 54*, 5788−5792.
48. Zaman, G. J. R., Flens, M. J., Van Leusden, M. R., De Haas, M., Mulder, H. S., Lankelma, J., Pinedo, H. M., Scheper, R. J., Baas, F., Broxterman, H. J., and Borst, P. (1994) *Proc. Natl. Acad. Sci. U.S.A. 91*, 8822−8826.
49. Ausubel, F. M., Brent, R., Kingston, R. E., Moore, D. D., Seidman, J. G., Smith, J. A., and Struhl, K. (1997) *Current Protocols in Molecular Biology*, John Wiley and Sons, New York.
50. Kozak, M. (1989) *Mol. Cell Biol. 9*, 5073−80.
51. Skehan, P., Storeng, R., Scudiero, D., Monks, A., McMahon, J., Vistica, D., Warren, J. T., Bokesch, H., Kenney, S., and Boyd, M. R. (1990) *J. Natl. Cancer Inst. 82*, 1107−1112.
52. Diah, S. K., Smitherman, P. K., Aldridge, J., Volk, E. L., Schneider, E., Townsend, A. J., and Morrow, C. S. (2001), *Cancer Res. 61*, 5461−5467.
53. Tietze, F. (1969) *Anal. Biochem. 27*, 502−522.
54. Cox, B., Murphey, L. J., Zackert, W. E., Chinery, R., Graves-Deal, R., Boutaud, O., Oates, J. A., Coffey, R. J., and Morrow, J. D. (2002) *Biochim. Biophys. Acta Mol. Cell Biol. Lipids 1584*, 37−45.
55. Paumi, C. M., Ledford, B. G., Smitherman, P. K., Townsend, A. J., and Morrow, C. S. (2001) *J. Biol. Chem. 276*, 7952−7956.
56. Morrow, C. S., Smitherman, P. K., Diah, S. K., Schneider, E., and Townsend, A. J. (1998) *J. Biol. Chem. 273*, 20114−20.
57. Zeng, H., Chen, Z. S., Belinsky, M. G., Rea, P. A., and Kruh, G. D. (2001) *Cancer Res. 61*, 7225−32.
58. Kool, M., van der Linden, M., de Haas, M., Scheffer, G. L., de Vree, J. M., Smith, A. J., Jansen, G., Peters, G. J., Ponne, N., Scheper, R. J., Elferink, R. P., Baas, F., and Borst, P. (1999) *Proc. Natl. Acad. Sci. U.S.A. 96*, 6914−9.
59. Hooijberg, J. H., Broxterman, H. J., Kool, M., Assaraf, Y. G., Peters, G. J., Noordhuis, P., Scheper, R. J., Borst, P., Pinedo, H. M., and Jansen, G. (1999) *Cancer Res. 59*, 2532−5.

BI027347U